Calculation of the Added Mass and Damping Forces on Supercavitating Bodies

J.S. Uhlman, N.E. Fine and D.C. Kring

Engineering Technology Center, a Division of Anteon Corporation, Middletown, RI 02842

Abstract

A linearized formulation for the unsteady forces experienced by supercavitating bodies is developed in terms of their added mass and damping coefficients. The formulation is general, but is applied here using an axisymmetric base flow. Expressions for the added mass, damping and restoring tensors are derived in a form suitable for incorporation in a numerical "flight" simulation tool for supercavitating vehicles. Disk and conical cavitating bodies are investigated. It is found that the added mass in surge can actually be negative for small values of the reduced frequency. The physical interpretation of this phenomenon is provided.

1 Introduction

A fully wetted body moving in an unsteady manner in an inviscid fluid experiences an inertial force due to the acceleration of the fluid by the body. That force is generally referred to as the added mass force since it can be expressed as the product of a coefficient with units of mass and the acceleration of the body. Also, since independent mass coefficients exist for each direction of acceleration, one may define an added mass tensor that in turn depends only on the body geometry. The added mass tensor may then be used in the equations of motion of the body, which can be used in the design of guidance and control algorithms.

Current interest in the development of supercavitating high-speed vehicles has led to the development of guidance and control algorithms for supercavitating bodies (Kirschner, et al, 2001). However, memory effects complicate computation of the hydrodynamic coefficients when part of the body is enveloped by a gas-filled cavity. The added mass tensor for fully wetted bodies is independent of the motion history of the body, and incorporating the added mass effects in the equations of motion is simple. In contrast, for supercavitating bodies, the shape and extent of the cavity depends on the history of the body motion. It follows that the forces experienced by a supercavitating vehicle undergoing unsteady motion should also depend on the history of the body motion.

In this work, we seek to quantify the forces experienced by supercavitating non-lifting bodies in an unsteady, irrotational flow of an inviscid and incompressible fluid. By defining an added mass tensor for supercavitating vehicles, we hope to find a simple and accurate approach to including unsteady inertial forces in their equations of motion. Our approach is to formulate the unsteady problem as a perturbation of a steady basis flow, and to solve for the unsteady flow in the frequency domain. This approach bears great similarity to that taken in previous works in solving the problem of ship motions in a seaway. For that reason, the formulation presented here closely follows two seminal works on that subject: Timman and Newman (1962) and Ogilvie and Tuck (1969).

2 Formulation

Consider a supercavitating body, such as the one shown in figure 1, undergoing nominally steady forward motion with velocity U_0 in the negative x direction. We seek expressions for the added mass and damping forces experienced by the body in response to unsteady motions, which will be assumed to be small relative to the forward speed. We will formulate the boundary value problem using a Cartesian coordinate system $\vec{x} = (x, y, z)$ fixed on the vehicle. The fluid is assumed to be inviscid and incompressible and the flow irrotational, so that the flow field may be written as the gradient of a potential, $\Phi(\vec{x}, t)$, which satisfies Laplace's equation:

$$\nabla^2 \Phi = 0 . \tag{1}$$

The fluid velocity consists of an unsteady perturbation superposed on a steady mean flow. Accordingly, the velocity potential is decomposed into a steady mean velocity potential and an unsteady perturbation potential:

$$\Phi(\vec{x}, t) = \Phi_0(\vec{x}) + f(\vec{x}, t) . \tag{2}$$

2.1 Kinematic Boundary Condition

If the body and cavity surface is represented by the function $F(\vec{x}, t)$, then the exact potential flow kinematic boundary condition to be satisfied on the surface is:

$$\frac{DF}{Dt} = \frac{\partial F}{\partial t} + \nabla(\Phi_0 + f) \cdot \nabla F = 0 . \tag{3}$$

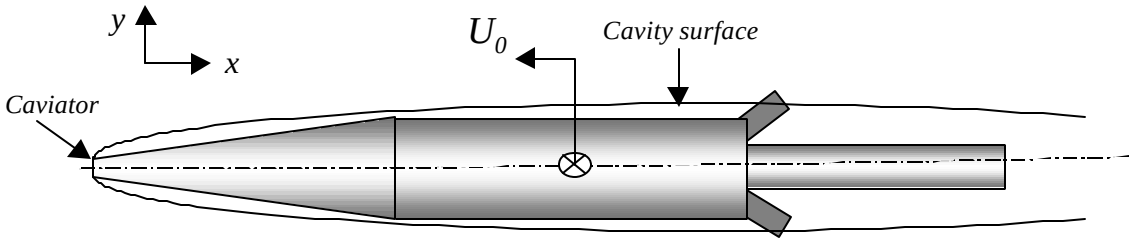

Figure 1 Notional sketch of a supercavitating vehicle.

The position of the surface may be defined as the sum of the steady mean position, $\vec{x}_0 = (x_0, y_0, z_0)$, and a small unsteady displacement:

$$\vec{x} = \vec{x}_0 + \vec{x}(x,t) \,. \tag{4}$$

Using this definition, the time derivative and gradient of *F* may be written as follows:

$$\frac{\partial F}{\partial t} = -\frac{\partial \vec{x}}{\partial t}\cdot\nabla_{x_0} F$$

$$\nabla F = \nabla_{x_0} F - \hat{i}\frac{\partial \vec{x}}{\partial x}\cdot\nabla_{x_0} F - \hat{j}\frac{\partial \vec{x}}{\partial y}\cdot\nabla_{x_0} F - \hat{k}\frac{\partial \vec{x}}{\partial z}\cdot\nabla_{x_0} F$$

where the subscript "x_0" denotes that the gradient operator is to be evaluated on the mean position of the body, with $\vec{x} = \vec{x}_0$. The unit vectors in the x_0, y_0 and z_0 coordinate directions are $\hat{i}, \hat{j}$ and $\hat{k}$, respectively. Substituting these expressions in equation (3), the kinematic boundary condition becomes:

$$-\frac{\partial \vec{x}}{\partial t}\cdot\nabla_{x_0} F + \nabla(\Phi_0 + f)\cdot\left(\nabla_{x_0} F - \hat{i}\frac{\partial \vec{x}}{\partial x}\cdot\nabla_{x_0} F - \hat{j}\frac{\partial \vec{x}}{\partial y}\cdot\nabla_{x_0} F - \hat{k}\frac{\partial \vec{x}}{\partial z}\cdot\nabla_{x_0} F\right) = 0 \tag{5}$$

Equation (5) applies on the exact body surface $F(\vec{x}, t)$. This expression may be linearized under the assumption that the unsteady displacement amplitudes, the perturbation potential and its spatial derivatives are all small. Using a Taylor expansion for the velocity field

$$\nabla(\Phi_0 + f) = \nabla_{x_0}\Phi_0 + \vec{x}\cdot\nabla_{x_0}(\nabla_{x_0}\Phi_0) + \nabla_{x_0} f + O(x^2) \tag{6}$$

we may recast equation (5) as follows:

$$-\frac{\partial \vec{x}}{\partial t}\cdot\nabla_{x_0} F + \left(\nabla_{x_0}\Phi_0 + \vec{x}\cdot\nabla_{x_0}(\nabla_{x_0}\Phi_0) + \nabla_{x_0} f\right)\cdot\left(\nabla_{x_0} F - \hat{i}\frac{\partial \vec{x}}{\partial x}\cdot\nabla_{x_0} F - \hat{j}\frac{\partial \vec{x}}{\partial y}\cdot\nabla_{x_0} F - \hat{k}\frac{\partial \vec{x}}{\partial z}\cdot\nabla_{x_0} F\right) + O(x^2) = 0 \,. \tag{7}$$

Rearranging terms, the unsteady components of equation (7) become:

$$\nabla_{x_0} f\cdot\nabla_{x_0} F = \frac{\partial \vec{x}}{\partial t}\cdot\nabla_{x_0} F + \left(\nabla_{x_0}\Phi_0\cdot\nabla_{x_0}\vec{x} - \vec{x}\cdot\nabla_{x_0}(\nabla_{x_0}\Phi_0)\right)\cdot\nabla_{x_0} F + O(x^2) \,. \tag{8}$$

Noting that $\nabla_{x_0} F$ is normal to the body/cavity surface, equation (8) reduces to

$$\frac{\partial f}{\partial n} = \frac{\partial \vec{x}}{\partial t}\cdot\hat{n} + \left(\nabla_{x_0}\Phi_0\cdot\nabla_{x_0}\vec{x} - \vec{x}\cdot\nabla_{x_0}(\nabla_{x_0}\Phi_0)\right)\cdot\hat{n} \,. \tag{9}$$

Equation (9) is the linearized kinematic boundary condition to be applied on the mean body/cavity surface.

We now consider only the wetted portion of the boundary and assume that its motion is associated with rigid-body motion of the vehicle. The displacement amplitude may be expressed as the sum of a rigid body translation, $\vec{x}_T$, and rotation, $\vec{x}_R$:

$$\vec{x} = \vec{x}_T + \vec{x}_R \times \vec{x}_0 \,. \tag{10}$$

Decomposing the perturbation potential into a sum of components proportional to complex harmonic displacement amplitudes,

$$f = z_j j_j(\vec{x}_0) e^{iwt}, \tag{11}$$

where summation over repeated indices is implied and where the magnitudes of the complex amplitudes are

$$\begin{aligned}(z_1, z_2, z_3) &= \vec{x}_T \\ (z_4, z_5, z_6) &= \vec{x}_R,\end{aligned} \tag{12}$$

and substituting in equation (9) yields:

$$\frac{\partial j_j(\vec{x}_0)}{\partial n} = iwn_j + m_j. \tag{13}$$

In (13), the generalized normal and so-called "m-terms" are given by (Ogilvie and Tuck, 1969):

$$\begin{aligned}(n_1, n_2, n_3) &= \hat{n} \\ (n_4, n_5, n_6) &= \vec{x}_0 \times \hat{n} \\ (m_1, m_2, m_3) &= -\hat{n} \cdot \nabla_{x_0}\left(\nabla_{x_0}\Phi_0(\vec{x}_0)\right) \\ (m_4, m_5, m_6) &= -\hat{n} \cdot \nabla_{x_0}\left(\vec{x}_0 \times \nabla_{x_0}\Phi_0(\vec{x}_0)\right).\end{aligned} \tag{14}$$

Equation (13) is the linearized kinematic boundary condition to be applied on the wetted portion of the body for each mode of oscillation, j=1,..,6.

2.2 Dynamic Boundary Condition

To derive the linearized dynamic boundary condition, we start with the following form of Bernoulli's equation:

$$r\frac{\partial \Phi(\vec{x}, t)}{\partial t} + \tfrac{1}{2} r \nabla\Phi(\vec{x}, t) \cdot \nabla\Phi(\vec{x}, t) = \left(p_\infty - p_c\right) + \tfrac{1}{2} r U_0^2 \tag{15}$$

where p_∞ and p_c are the pressure at infinity and in the cavity, respectively, and where buoyant effects are ignored. Inserting the decomposition of the total potential given in equation (2) and the Taylor expansion of its gradient from equation (6), this becomes:

$$\begin{aligned}2\frac{\partial f(\vec{x}_0, t)}{\partial t} + \left(\nabla_{x_0}\Phi_0(\vec{x}_0) + \vec{x} \cdot \nabla_{x_0}(\nabla_{x_0}\Phi_0(\vec{x}_0)) + \nabla_{x_0} f(\vec{x}_0, t)\right) \cdot \left(\nabla_{x_0}\Phi_0(\vec{x}_0) + \vec{x} \cdot \nabla_{x_0}(\nabla_{x_0}\Phi_0(\vec{x}_0)) + \nabla_{x_0} f(\vec{x}_0, t)\right) \\ = U_0^2(1+s)\end{aligned} \tag{16}$$

where the cavitation number is defined as follows:

$$s = \frac{p_\infty - p_c}{\frac{1}{2} r U_0^2}.$$

Keeping only terms linear in x, equation (16) reduces to

$$2\frac{\partial f(\vec{x}_0, t)}{\partial t} + \nabla_{x_0}\Phi_0(\vec{x}_0) \bullet \nabla_{x_0}\Phi_0(\vec{x}_0) + 2\nabla_{x_0}\Phi_0(\vec{x}_0) \bullet \nabla_{x_0} f(\vec{x}_0, t) + 2\nabla_{x_0}\Phi_0(\vec{x}_0) \bullet \left(\vec{x} \bullet \nabla_{x_0}(\nabla_{x_0}\Phi_0(\vec{x}_0))\right) = U_0^2(1+s) \tag{17}$$

The steady potential, $\Phi_0(\vec{x}_0)$, is assumed to satisfy the steady dynamic boundary condition:

$$\nabla_{x_0}\Phi_0(\vec{x}_0) \cdot \nabla_{x_0}\Phi_0(\vec{x}_0) = U_0^2(1+s) \quad \text{on the cavity} \tag{18}$$

so that equation (17) yields

$$\frac{\partial f(\vec{x}_0, t)}{\partial t} + \nabla_{x_0}\Phi_0(\vec{x}_0) \cdot \nabla_{x_0} f(\vec{x}_0, t) + \nabla_{x_0}\Phi_0 \cdot \left(\vec{x} \cdot \nabla_{x_0}\left(\nabla_{x_0}\Phi_0(\vec{x}_0)\right)\right) = 0 \tag{19}$$

The last term on the left-hand-side of equation (19) may be evaluated as follows:

$$\nabla_{x_0}\Phi_0 \cdot \left(\vec{x} \cdot \nabla_{x_0}(\nabla_{x_0}\Phi_0)\right) = \vec{x} \cdot \left(\nabla_{x_0}(\nabla_{x_0}\Phi_0) \cdot \nabla_{x_0}\Phi_0\right) = \tfrac{1}{2}\vec{x} \cdot \nabla_{x_0}\left(\nabla_{x_0}\Phi_0 \cdot \nabla_{x_0}\Phi_0\right) = 0. \tag{20}$$

This term vanishes on S_C because the last bracketed term of (20) is constant, as defined in equation (18).

Substituting the decomposition of the perturbation potential, equation (11), in equation (19) and making use of equation (20) results in the following linearized dynamic boundary condition:

$$iwj_j(\vec{x}_0) + \nabla\Phi_0(\vec{x}_0) \cdot \nabla j_j(\vec{x}_0) = 0 \quad \text{on the cavity, } j = 1,...,6. \tag{21}$$

Equation (21) will be applied on the steady mean cavity surface, S_C.

2.3 Cavity Termination

The need for a termination model arises from the inconsistency inherent in forcing a constant-pressure streamline to end at a stagnation point. In this effort, a re-entrant jet cavity termination model is employed, as shown in figure 2. This termination model was originally devised by Efros (1946) and Kreisel (1946). Details of the numerical implementation in the boundary element method may be found in Uhlman (2001).

2.4 Boundary Integral Equation

The perturbation potential satisfies Green's third identity:

$$2p f(\vec{x},t) + \iint_S \left[f(\vec{y},t) \frac{\partial}{\partial n}\big(G(\vec{x},\vec{y})\big) - G(\vec{x},\vec{y}) \frac{\partial}{\partial n}\big(f(\vec{y},t)\big) \right] dS = 0 \tag{22}$$

where the Green's function, G, is given by

$$G(\vec{x},\vec{y}) = \frac{1}{|\vec{x}-\vec{y}|} \tag{23}$$

and where the field point, $\vec{x}$, lies on the boundary. Substituting the decomposition (11) and noting that the complex amplitudes, z_j, have no spatial dependence, we find that each complex potential, j_j, satisfies

$$2p j_j(\vec{x}) + \iint_S \left[j_j(\vec{y}) \frac{\partial G(\vec{x},\vec{y})}{\partial n} - G(\vec{x},\vec{y}) \frac{\partial j_j(\vec{y})}{\partial n} \right] dS = 0 . \tag{24}$$

The boundary conditions to be satisfied are the kinematic boundary condition (equation (13)), which defines the source distribution $\partial j_j / \partial n$ on the wetted portion of the body, and the dynamic boundary condition (equation (21)) which defines the dipole distribution j_j on the cavity. Inserting the boundary conditions in (24) and rearranging the terms so that the known quantities are on the right-hand-side, we arrive at the following expression:

$$2p j_j + \iint_{S_{BW}} j_j(\vec{y}) \frac{\partial G(\vec{x},\vec{y})}{\partial n} dS - \iint_{S_C} \frac{\partial j_j(\vec{y})}{\partial n} G(\vec{x},\vec{y}) dS + \iint_{S_C+S_J} j_j(\vec{y}) \frac{\partial G(\vec{x},\vec{y})}{\partial n} dS = \iint_{S_{BW}} \{ iwn_j + m_j \} G dS . \tag{25}$$

Here, the wetted body surface is S_{BW}, the cavity surface is S_C and the jet face is S_J, as shown in figure 2.

2.5 Hydrodynamic Coefficients

Once the source and dipole distributions have been computed, the forces may be found by integrating the pressure over the wetted surface

$$F_i(t) = \iint_{S_B(t)} p(\vec{x},t) n_i dS . \tag{26}$$

In (26), $S_B(t)$ is the exact surface of the body. The unsteady pressure on $S_B(t)$ may be written

$$p(\vec{x},t) = -r \frac{\partial}{\partial t}\big(f(\vec{x},t)\big) - \tfrac{1}{2} r \nabla\big(\Phi_0(\vec{x}) + f(\vec{x},t)\big) \cdot \nabla\big(\Phi_0(\vec{x}) + f(\vec{x},t)\big) . \tag{27}$$

If we again introduce the intermediate coordinate system, $\vec{x}_0$, as in (4), equation (27) may be linearized for small x as follows:

$$p(\vec{x}_0,t) = -r \frac{\partial}{\partial t}\big(f(\vec{x}_0,t)\big) - r \nabla_{x_0}\Phi_0(\vec{x}_0) \cdot \nabla_{x_0} f(\vec{x}_0,t) - \tfrac{1}{2} r \vec{x} \cdot \nabla_{x_0}\left(\nabla_{x_0}\Phi_0(\vec{x}_0) \cdot \nabla_{x_0}\Phi_0(\vec{x}_0) \right) . \tag{28}$$

For the remainder of this paper, there will be no need to distinguish between the coordinates $\vec{x}$ and $\vec{x}_0$. It will be implicitly assumed that all quantities are defined relative to the steady mean coordinate system.

Inserting the decomposition (11) in (28) and the resulting expression in (26) then yields the following expression for the force (Nakos and Sclavounos, 1990):

$$F_i(t) = \mathrm{Re}\left\{ e^{iwt} \left[x_j \left(w^2 a_{ij} - iwb_{ij} - c_{ij} \right) \right] \right\} \tag{29}$$

where

$$a_{ij} = -\frac{r}{w^2}\,\mathrm{Re}\left\{\iint_{S_{B_0}}\left[iwj_j + \frac{\partial\Phi_0}{\partial x_k}\frac{\partial j_j}{\partial x_k}\right]n_i dS\right\} \tag{30}$$

$$b_{ij} = \frac{r}{w}\,\mathrm{Im}\left\{\iint_{S_{B_0}}\left[iwj_j + \frac{\partial\Phi_0}{\partial x_k}\frac{\partial j_j}{\partial x_k}\right]n_i dS\right\} \tag{31}$$

$$c_{ij} = r\,\mathrm{Re}\left\{\iint_{S_{B_0}}\left[x_k\cdot\frac{\partial}{\partial x_k}\left(\frac{1}{2}\frac{\partial\Phi_0}{\partial x_k}\frac{\partial\Phi_0}{\partial x_k}\right)\right]_j n_i dS\right\} \tag{32}$$

In equation (29), the force is written as a sum of added mass (a_{ij}), damping (b_{ij}) and restoring force (c_{ij}) tensors. The surface S_{B_0} is the steady mean body surface.

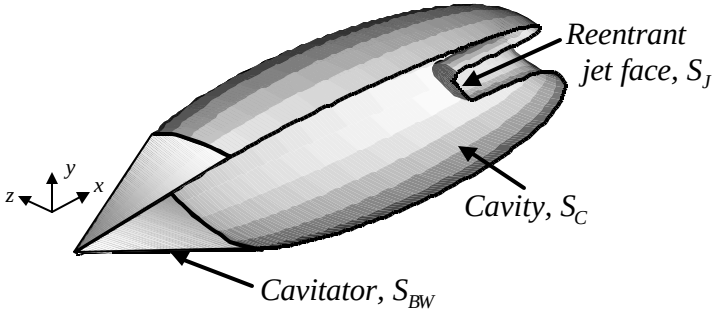

Figure 2 *Cut-away sketch of a supercavitating cone showing the various surface definitions.*

3 Numerical Implementation for an Axisymmetric Basis Flow

To this point, we have formulated the problem in terms of a general steady basis flow. To demonstrate the method, we now define our steady basis flow to be that of an axisymmetric cavitator with a reentrant jet cavity termination, as shown in figure 2. The axisymmetric flow is computed numerically via a low-order boundary element method (Uhlman, 2001). In the numerical solution of the basis flow, the cavity length is assumed to be known, and the cavitation number is determined as part of the solution. An iterative method is used to determine the cavity shape that satisfies the kinematic and dynamic boundary conditions. For further details of the method, the reader is referred to Uhlman (2001). For the remainder of the present paper, we limit our discussion to surge motions only. Heave and pitch motions have also been investigated, but will not be discussed here.

3.1 Boundary value problem

Noting that for an axisymmetric base problem we have

$$\nabla\Phi_0 = \frac{\partial\Phi_0}{\partial s}\hat{e}_s = U_0\sqrt{1+s}\,\hat{e}_s \tag{33}$$

where s and $\hat{e}_s$ are the arclength and unit vector along a meridian, we find that the dynamic boundary condition on S_C (equation (21)) becomes:

$$iwj_j + U_0\sqrt{1+s}\,\frac{\partial j_j}{\partial s} = 0 \ \text{ on } \ S_C\,. \tag{34}$$

Equation (34) may be integrated to yield

$$j_j = j_{0_j}e^{-ig(s)} \tag{35}$$

where

$$g(s) = \frac{w}{U_0\sqrt{1+s}}\left(s - s_0\right) \tag{36}$$

and where j_0 is the value of j_j at $s = s_0$. For convenience, we will drop the subscript *j*, with the understanding that *j=1* for the remainder of the paper. The dynamic boundary condition on the jet cross-section is

$$iwj + \frac{\partial \Phi_0}{\partial n}\frac{\partial j}{\partial n} = 0 \text{ on } S_J . \tag{37}$$

Noting that, on the jet cross section, $\partial\Phi_0/\partial n = U_0\sqrt{1+s}$, equation (37) becomes

$$\frac{\partial j}{\partial n} = -\frac{iw}{U_0\sqrt{1+s}} j_0 e^{-ig(s_J)} \tag{38}$$

where s_J is the arclength along the cavity to the edge of the jet cross section and. where we've assumed that $\partial j/\partial s$ is zero on the jet face.

On the wetted part of the body, S_{BW}, Green's third identity becomes:

$$2p\, j + \int_{S_{BW}} j\,\frac{\partial G}{\partial n}ds - \int_{S_C}\frac{\partial j}{\partial n}Gds + j_0\left\{\int_{S_C+S_J} e^{-ig(s)}\frac{\partial G}{\partial n}ds + \frac{ike^{-ig(s_J)}}{d\sqrt{1+s}}\int_{S_J} Gds\right\} = \int_{S_{BW}}\{iwn+m\}Gds \tag{39}$$

and on the cavity

$$2p\, j_0 e^{-ig(s)} + \int_{S_{BW}} j\,\frac{\partial G}{\partial n}ds - \int_{S_C}\frac{\partial j}{\partial n}Gds + j_0\left\{\int_{S_C+S_J} e^{-ig(s)}\frac{\partial G}{\partial n}ds + \frac{ike^{-ig(s_J)}}{d\sqrt{1+s}}\int_{S_J} Gds\right\} = \int_{S_{BW}}\{iwn+m\}Gds \tag{40}$$

where d is the body diameter at the cavity detachment location and where we have defined the reduced frequency, $k = wd/U_0$.

3.2 Results

In this section, we present added mass and damping results for the circular disk, a conical cavitator with various half-angles, and a roundnose conical cavitator. For the present paper, we consider only surge motions. Results for heave and pitch motions will be presented in a separate publication.

Figure 3 shows the convergence of the added mass for a roundnose conical cavitator in surge with increasing number of panels. The shape of the cavitator is shown in figure 3a and the convergence is shown in figure 3b. The total number of panels used to discretize the boundary is NBOD+NCAV+NJET, where NBOD is the number of panels on the cavitator, NCAV is the number of panels representing the cavity, and NJET is the number of panels representing the jet face. The steady cavity length is five cavitator base diameters, corresponding to a cavitation number of $s \approx 0.19$. The corresponding convergence of the cavitation number is also shown in the figure.

Figure 4 shows the surge added mass and damping for the circular disk as a function of reduced frequency. As expected, the added mass asymptotes to a value close to half the theoretical value for the fully wetted disk at high reduced frequency. A surprising aspect of the result presented in figure 3 is the fact that the added mass takes on negative values for a range of reduced frequencies for $k \lesssim 3$. This result will be discussed in Section 3.3.

Figure 5 shows the added mass and damping for conical cavitators with half-angles of 30º, 45º and 60º, as well the results for the circular disk (e.g., 90º cone). The steady cavity length for each case is *L/d*=5, and the corresponding cavitation numbers are 0.183, 0.217 0.241, and 0.268, respectively. Note that, similar to the results for the disk, the added mass is negative for small reduced frequencies. However, as the half-angle increases, the level of the negative added mass decreases. For clarity, the added mass has been multiplied by the ratio $k^2/1+k^2$ in figure 5.

3.3 Discussion

As shown in figure 4, the added mass in surge can take on negative values over a range of reduced frequencies. This result is surprising, since it implies that the added mass force can reinforce the motion of the body. The result is also important, since the occurrence of negative added mass can effect the stability of a high speed supercavitating vehicle.

The physical explanation of the phenomena is as follows. When the cavitator moves in oscillatory surge, vorticity is shed at the base of the cavitator with every half-cycle of motion. The vorticity is then advected along the cavity boundary and out of the fluid domain via the reentrant jet. At any given moment, each element of shed vorticity on the cavity boundary induces an axial velocity at the cavitator in a direction that either opposes or coincides with the direction of motion of the cavitator. The axial velocity induced by the vorticity shed during the current half-cycle of motion coincides with the direction of motion. For motions with low reduced frequency, the

most recent element of shed vorticity contributes most of the induced velocity. Therefore, the net induced velocity contributes to the acceleration of the fluid, and therefore results in a negative added mass. However, for motions with high reduced frequencies, the shed vortices are more closely spaced so that the net induced axial velocity over the cavitator is greatly reduced. At high reduced frequencies there is no net induced axial velocity and the added mass is positive as expected.

It should be noted that an analogous phenomena occurs for fully-wetted hydrofoils undergoing small oscillatory heave motions. In that case, the shed vorticity is advected along the wake of the foil and induces a net vertical velocity in the direction of motion. This behavior is evident in the classical Theodorsen linear theory for unsteady hydrofoil motion (see e.g., Newman, 1986).

4 Conclusions

A method for computing the force coefficients for supercavitating bodies has been described. The method assumes harmonic oscillations and solves a linearized boundary value problem in the frequency domain for small perturbations to a steady basis flow. The method has been demonstrated for unsteady surge of axisymmetric cavitators. The numerical solution has been found to converge with increasing number of panels. It has been found that the added mass of the circular disk asymptotes to approximately half the theoretical value for fully wetted disks at high reduced frequencies. At low reduced frequencies, however, the added mass is actually negative. The physical explanation for this phenomenon was provided.

In future development of the method, we will include heave and pitch motions for axisymmetric flows, we will study the impact of the results on the stability of supercavitating bodies, and the method will be implemented for non-axisymmetric flows, including flows with lift.

Acknowledgements

This research was supported by Dr. Kam Ng of the Office of Naval Research (Contract No. N00014-00-C-0182). The authors are indebted to Dr. Ivan Kirschner for participating in discussions on this problem and for providing figure 1 of this report.

References

Efros, A. G. (1946), "Hydrodynamic Theory of Two-Dimensional Flow with Cavitation", *Dokl. Acad. Nauk. SSSR*, 51, pp 267-270.

Kirschner, I.N. , N.E. Fine, J.S. Uhlman and D.C. Kring (2001) , "Numerical Modeling of Supercavitating Flows", RTO AVT/VKI Special Course in Supercavitating Flows, Feb. 12-16.

Kreisel, G. (1946), "Cavitation with Finite Cavitation Numbers", Technical Report No. R1/H/36, Admiralty Res. Lab.

Nakos, D. E. and P.D. Sclavounos (1990), "Ship Motions by a Three Dimensional Rankine Panel Method", *18th Naval Hydrodynamics Conference, Ann Arbor, MI*.

Newman, J.N. (1986), Marine Hydrodynamics, MIT Press, Cambridge, MA.

Ogilvie, T.F. and E.O. Tuck, (1969), "A Rational Strip Theory for Ship Motions – Part I", Report No. 013, Dept. of Naval Architecture and Marine Engineering, University of Michigan, USA.

Timman, R. and J.N. Newman, (1962), "The Coupled Damping Coefficients of Symmetric Ships", *Journal of Ship Research*, 5(4), pp 34-55.

Uhlman, J.S., (1987), "The Surface Singularity Method Applied to Partially Cavitating Hydrofoils", *Journal of Ship Research*, 31(2).

Uhlman, J.S., (2001), "A Note on the Development of a Nonlinear Axisymmetric Reentrant Jet Cavitation Model", *ETC Technical Report No.* ETC:RPT:101497/-(U).

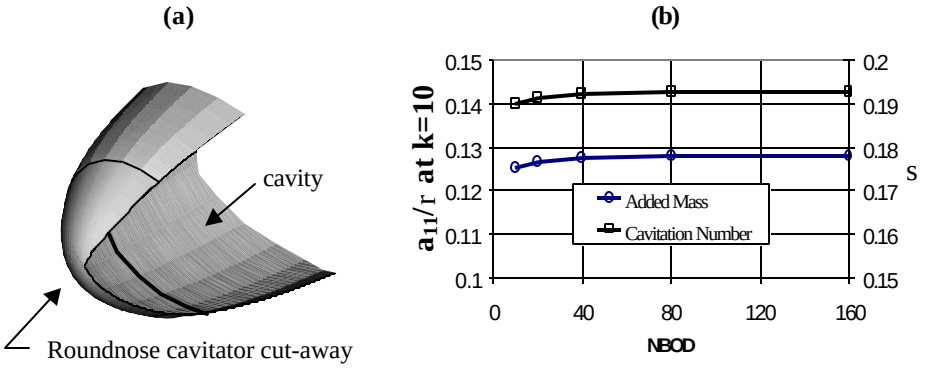

NBOD	NCAV	NJET
10	89	5
20	178	10
40	356	20
80	712	40
160	1424	80

Figure 3. *Convergence of surge added mass at k=10 and cavitation number for a roundnose conical cavitator with L/d=5.0 and NBOD=10, 20, 40, 80 and 160. The adjacent table shows the corresponding values of NCAV, NJET.*

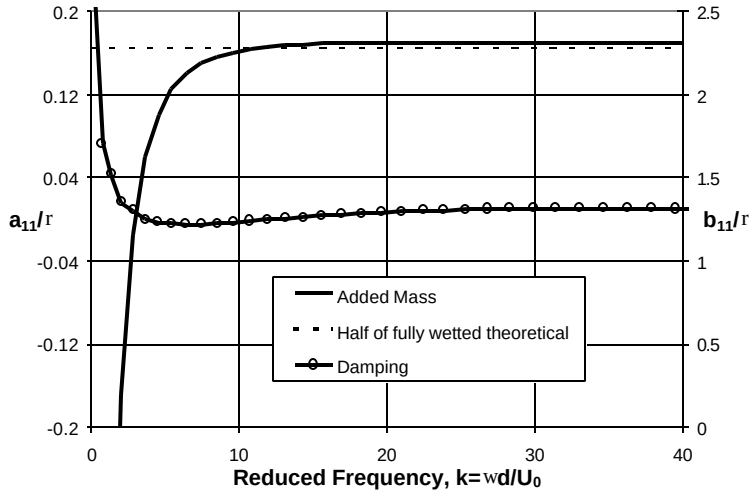

Figure 4. *Asymptotic behavior of the surge added mass for a circular disk at high reduced frequency, compared to half the theoretical value for a fully wetted disk.*

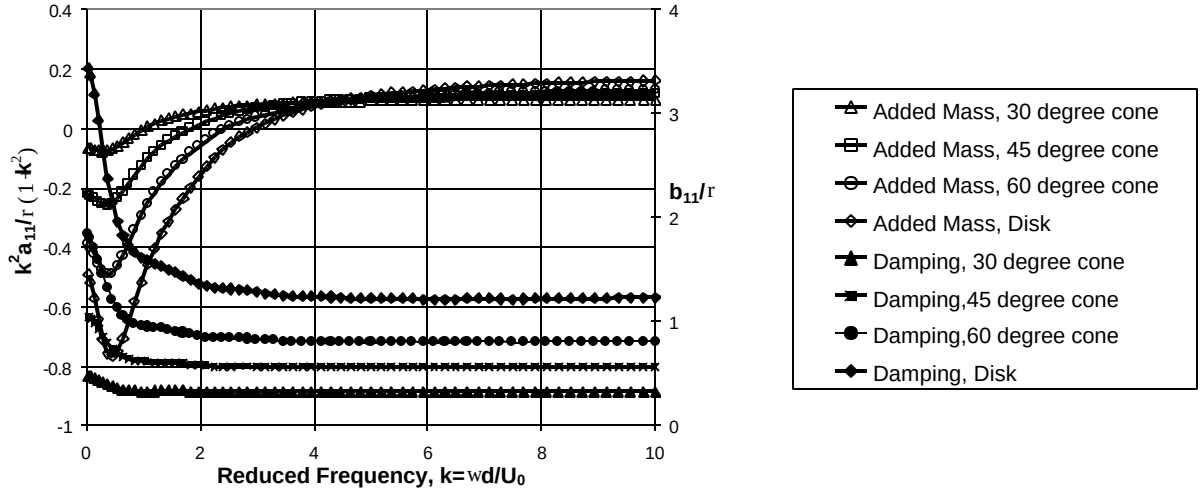

Figure 5. *Added mass and damping as a function of reduced frequency and cone half-angle for a conical cavitator. The cavity length is held fixed at L/d=5.*